Mine Water and the Environment (2022) 41:504–517
https://doi.org/10.1007/s10230-022-00861-y

TECHNICAL ARTICLE

Hydrogeochemical Processes of Carboniferous Limestone Groundwater in the Yangzhuang Coal Mine, Huaibei Coalfield, China

Jie Zhang[1] · Luwang Chen[1] · Xiaowei Hou[1] · Xingxing Ren[1] · Jun Li[1] · Yifei Chen[1]

Received: 5 May 2021 / Accepted: 1 March 2022 / Published online: 16 March 2022

Abstract

We examined the primary mechanisms controlling water quality evolution in the Carboniferous aquifer in the Yangzhuang coal mine (Huaibei coalfield). Q-mode factor analysis explained how the Na^+ and SO_4^{2-} concentrations gradually increase and the hydrochemical type transforms from Ca-HCO_3 to Ca·Na-HCO_3 and Ca·Na-HCO_3·SO_4 along the flow path. The high bicarbonate concentration appears to be due to dissolution of calcite and dolomite and an open carbonate system, while frequent water inrushes and the declining water level provide evidence for the relative closure of the Carboniferous limestone aquifer. Gypsum dissolution is the main SO_4^{2-} source. Inverse geochemical modeling sufficiently explained the hydrogeochemical processes that control the water quality evolution. These findings should aid the interpretation of groundwater hydrochemical evolution and groundwater quality management in the study area and other north China coalfields.

Keywords Hydrogeochemistry, · Carboniferous limestone aquifer · Multivariate statistical analysis · Water–rock interactions · Inverse modeling

Introduction

Coal is still China's major energy source, accounting for 57.7% of the country's primary energy consumption in the year 2019 (National Bureau of Statistics 2019). In north China, groundwater is the main source of drinking water for local residents (Liang et al. 2018; Lin et al. 2019; Liu and Sun 2011; Ma et al. 2011; Qiao et al. 2019). According to official data, north China's freshwater supply in 2019 was 83.85 billion m^3 (Ministry of Water Resources of China 2019). North China has become an important coal-producing area because of its rich widely distributed coal resources, and most of the coal mines are underground operations (Han et al. 2013; Liu et al. 2019a). Large-scale underground mining activities will inevitably affect the flow path of groundwater at different depths and change the hydraulic connection among different aquifers, which complicates the mining area's hydrogeological conditions. Unfortunately, there are frequent conflicts between coal mining and groundwater resource management, and the detrimental effects of coal mining on water resources have been fully demonstrated worldwide (Adam and Paul 2000; Andreas and Nikola 2011; Bridge 2004; Johnson and Younger 2006; Liang et al. 2018; Qiao et al. 2019; Younger and Wolkersdorfer 2004). Approximately 40% (2.7 Gm^3) of China's groundwater has been affected by mining activities (Hu and Yan 2000; Liang et al. 2018; Zhang et al. 2020a). Therefore, fully understanding the source and evolution of groundwater during is important for the protection and utilization of the region's groundwater resources.

Mine safety has always been a serious issue in China because of the potential inrush of groundwater at the working face or tunnel face during the mining of deep coal seams (Chen et al. 2016; Gui et al. 2017; Wu et al. 2014; Yin et al. 2019; Zhang 2005). A typical limestone aquifer in the north China coalfield, called the Carboniferous limestone aquifer, is not only the key drinking water source for residents, but is also a critical threat to mining activity in terms of its water-inrush disaster potential. Under normal circumstances, this is located below the Permian coal seams; thus, the water inrush caused by this aquifer is called an underlying aquifer disaster (Gui et al. 2017; Shi et al. 2019; Wu et al. 2017). Groundwater extraction can mitigate this risk to a certain extent; however, this can lead to a series of concomitant issues, such as land subsidence, mine collapse, and

✉ Luwang Chen
luwangchen8888@163.com

[1] School of Resources and Environmental Engineering, Hefei University of Technology, Hefei 230009, China

the unnatural inducement of water from neighboring water-resource aquifers and even the ground surface (Qiao et al. 2019; Salmi et al. 2017; Unlu et al. 2013).

The evolution of groundwater chemistry in coal mining regions is mainly affected by natural processes (groundwater flow conditions, water–rock interactions) and anthropogenic activities (coal mine industrial production, drainage of mine water). However, for a particular area, it is generally stable. Meanwhile, coal mines regularly monitor the hydrochemical compositions of groundwater in different aquifers for safety purposes. Therefore, fully understanding the hydrochemical evolution of the Carboniferous groundwater in the study area can help enhance mine safety and sustainable groundwater resource development.

The hydrogeochemical evolution of the groundwater system has been extensively investigated in recent years (Binet et al. 2016; Cortes et al. 2016; Gastmans et al. 2010; Liu et al. 2017; Shen et al. 1999; Zhang et al. 2020b). Different methods, such as hydrogeochemical analysis, multivariate statistics, isotope analysis, laboratory column simulation, and hydro-geochemical modeling, have been widely used to identify the origins, hydrogeochemical processes, and transportation of chemical substances of regional and local groundwater systems (Adhikari and Mal 2019; Carucci et al. 2012; Dogramaci et al. 2017; Güler et al. 2002; Kanduč et al. 2014; Li et al. 2018; Liu et al. 2019a, b, 2020; Moya et al. 2016; Qiao et al. 2019; Sefie et al. 2018; Sun et al. 2017; Trabelsi and Zouari 2019; Zhang et al. 2020b, 2021; Zheng et al. 2019). Most previous studies suggested that analysis of the relationship between major ions and minerals was useful to interpret the processes controlling the hydrogeochemical evolution. Moreover, multivariate statistical analysis and geochemical models were the most widely applied methods for hydrogeochemical analysis (Güler et al. 2002, 2012; Liu et al. 2017, 2020; Qian et al. 2018; Qiao et al. 2019; Trabelsi and Zouari 2019; Zhang et al. 2020b, 2021). In north China, scholars also focused on the hydrogeochemical evolution of groundwater in coal mining districts. Popular methods, including groundwater ions, trace elements, and environmental isotopes, have also been widely used to accurately interpret the origin and the flow properties of both shallow and deep groundwater in these coalfields (Huang and Chen 2012; Liu et al. 2017, 2019a; Ma et al. 2011; Qian et al. 2016; Qu et al. 2018; Sun et al. 2017; Zhang et al. 2020b, 2021). Previous studies of the groundwater in the Huaibei coalfield mainly concentrated on mine safety issues induced by water inrush incidents (Chen et al. 2016, 2017; Gui et al. 2017; Zhang et al. 2020b, 2021) with minor description of groundwater evolution from the perspective of hydrogeochemical processes.

The Yangzhuang coal mine is an extremely hydrogeologically complex mine in the Huaibei coalfield that has experienced serious underlying aquifer disasters (Luo and Peng 2005; Wang et al. 2009). The Carboniferous groundwater in this area is the main drinking water source for residents, but is also a major threat to mine workers. Therefore, to ensure the quality of domestic water and safe coal production, we undertook to: determine the characteristics of the Carboniferous groundwater, expose potential water–rock interactions of the aquifer due to mining, and identify the processes controlling changes in the groundwater flow path from both hydrogeological and hydrogeochemical perspectives. Hydrogeochemical processes and transport paths in the Carboniferous limestone aquifer in the northern Huaibei area, Q-mode factor analysis, hydrogeochemical correlations analysis, and inverse geochemical modeling with mineral phase were all used.

Study Area

As stated above, this study focused on the hydrogeochemical process of underground water within the Yangzhuang coal mine in the Suixiao mining district of the Huaibei coalfield in Anhui Province, eastern China (Fig. 1). The land surface is a relatively flat alluvial plain with elevations ranging from + 29.2 to + 31.7 m above sea level. The region is characterized by a warm temperate semi-humid climate, with an average annual temperature of 14.4 ℃. The average annual precipitation is 854 mm, with 75% falling from June to August, while the average annual evaporation ranges from 1800 to 1900 mm (Yin et al. 2011; Zhang et al. 2021). The Sha, Dai, Long, and Sui Rivers flow through the region from east to west, respectively, as part of the Huai River system. The Yangzhuang mine started operating in the 1960s, with an average coal production of 2.1 million t/year. The main coal seams are the Permian no. 5 and no. 6 coals, with average burials depth of about − 500 m.

Similar to other coal mines in Huaibei coalfield, the strata in the study area, from top to bottom, are Quaternary, Permian, Carboniferous, and Ordovician, in which the main coal-bearing strata is Permian. Controlled by the Zhahe syncline structure, the thickness of the coal measures in the Yangzhuang mine increases along the direction of the alluvial plain. The geological structure in the area is dominated by folds with relatively poor development of faults. The axial direction of folds in this region are nearly SN. The four representative key aquifers from top to bottom (simplified) are the Quaternary loose sand aquifer (QLA), the Permian fractured sandstone aquifer (PSA), the Carboniferous Taiyuan Formation limestone aquifer group (CLA), and the deep and thickest Ordovician limestone aquifer (OLA), respectively. The burial depth of the QLA ranges from 15 to 80 m deep, with an average of 43.2 m. It is dominated by fine sand with 3–4 layers of sandy clay. The upper part of this aquifer is diving, whereas the lower part is confined water. The PSA

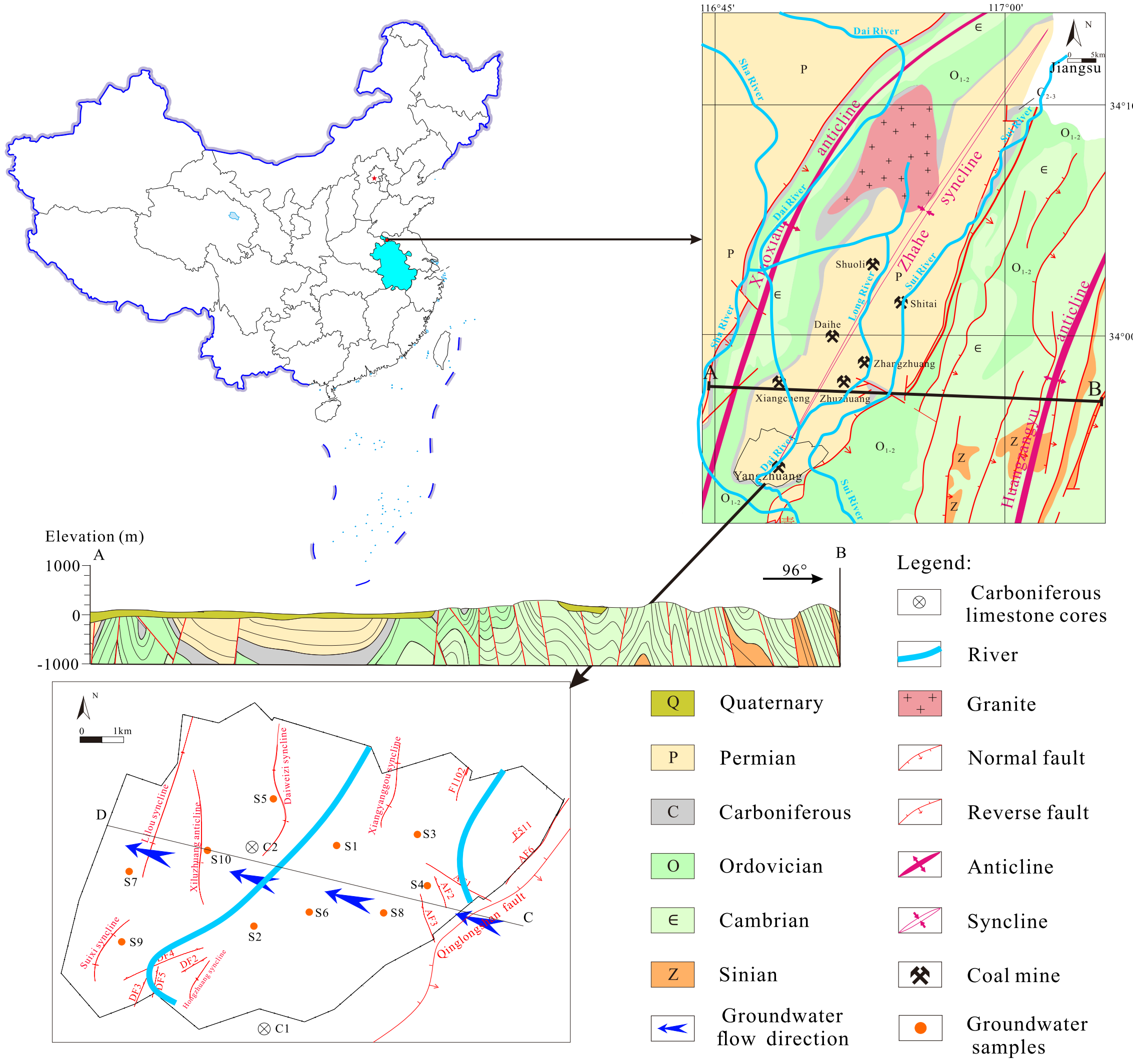

Fig. 1 Geographical location, geological map, and sampling distribution of the study area. **A**, **B** is the cross section of the northern part of the Huaibei coalfield, while **C**, **D** is the groundwater flow direction in the Yangzhuang coal mine

is 167.35 m thick with dominant components of medium-fine sandstone and magmatic rock and minor mudstone and sandy mudstone layers. The CLA, with an average thickness of 140 m, contains limestone, mudstone, fine sandstone, and thin coal seams; limestone accounts for most of the components. There are 12 layers of limestone from top to bottom; among them, four layers of limestone, named L_1, L_2, L_3, and L_4, respectively, are regarded as a unified aquifer, and were the object of this research. The OLA is 500 m thick and is mainly composed of dolomitic and argillaceous limestone. Both the PSA and CLA are frequent sources of water inrush but the CLA is also an important source of drinking water for residents.

A hill outcrop of OLA was found southeast of the coal mine, suggesting that the aquifer is recharged by atmospheric precipitation and is hydraulically connected with the CLA through the Qinglongshan reverse fault. Based on the hydrodynamic characteristics, groundwater in the CLA generally flows from the limestone outcrop in the southeast to the deep zone of the syncline structure in the northwest. Meanwhile, the CLA is a typical confined aquifer, and the water pressure is extremely high because of its abundant water content. Additionally, there is an aquiclude between the deep coal seam and the CLA, which is mainly composed of mudstone and siltstone, with an average thickness of about 50 m. Therefore, the potential flow direction will be from the lower aquifer (CLA) to the upper mining stopes and the PSA through natural faults and derived fractures. In other words, the PSA groundwater and mine drainage are unlikely to interfere with the CLA. The hydrogeological profile of the study area, as shown in Fig. 2, is similar to most of north China's coalfields.

The CLA is dominantly limestone. Previous studies indicate that the CaO/MgO ratio is between 14.9 and 68.9, with

an average value of 41 (Xue et al. 2014). Similar to other coal mines in north China, the potential water-reacting minerals in the CLA in the study area are mainly calcite, dolomite, gypsum, quartz, and halite.

Materials and Methods

Sample Collection and Analysis

In this study, 10 groundwater samples were collected in June 2018 from underground pumping holes and mining tunnels of the CLA during the mining period. All of the samples were sealed using polyolefin bottles. The containers were rinsed four or five times using the water to be sampled before the samples were collected. The samples were measured both on-field and in the lab to obtain the related data. Related parameters such as temperature (T/℃), pH, and total dissolved solids (TDS) were directly determined in the field using ST20 and ST20T-B handheld portable devices. Additionally, the residual water samples were then filtered on-site with a 0.45 μm filter for laboratory testing in the laboratory of National Coal Mine Flood Control Engineering Technology Research Center (Suzhou, China). Acid–base titration was used to determine the concentration of HCO_3^-. Na^+, Ca^{2+}, Mg^{2+}, Cl^-, and SO_4^{2-} were determined by ion chromatography (ICS-600–900).

Additionally, two cores from the CLA were collected and tested in the laboratory of the School of Resources and Environmental Engineering, Hefei University of Technology (Hefei, China), using an x-ray diffractometer (XRD) model DX-2700 (Rigaku, Japan) to predict the potential reactants.

Analytical Methods

Factor analysis is a multivariate statistical analysis method for data simplification (Huang and Chen 2012; Huang and Lu 2014; Szabó 2015). R-mode factor analysis is mainly used to reveal the relationship among different variables, while Q-mode factor analysis tries to determine the pattern or grouping of samples in "multivariate space" (Walden et al. 1992). When evaluating groundwater geochemistry, the relative compositions of the constituents for a given sample are often as important as their absolute concentrations (Davis 1973). The original data matrix can be transformed into a description of the "proportional index" to evaluate the similarity among different samples according to the proportion of sample components. Q-mode factor analysis forms a similarity matrix, which is composed of proportional similarity coefficients. The eigenvectors extracted from the similarity matrix are called loadings, which describe the proportion of each sample required to project variables onto the factor axis. In this study, Q-mode factor analysis was used to explore the internal relationship between the samples collected from the CLA.

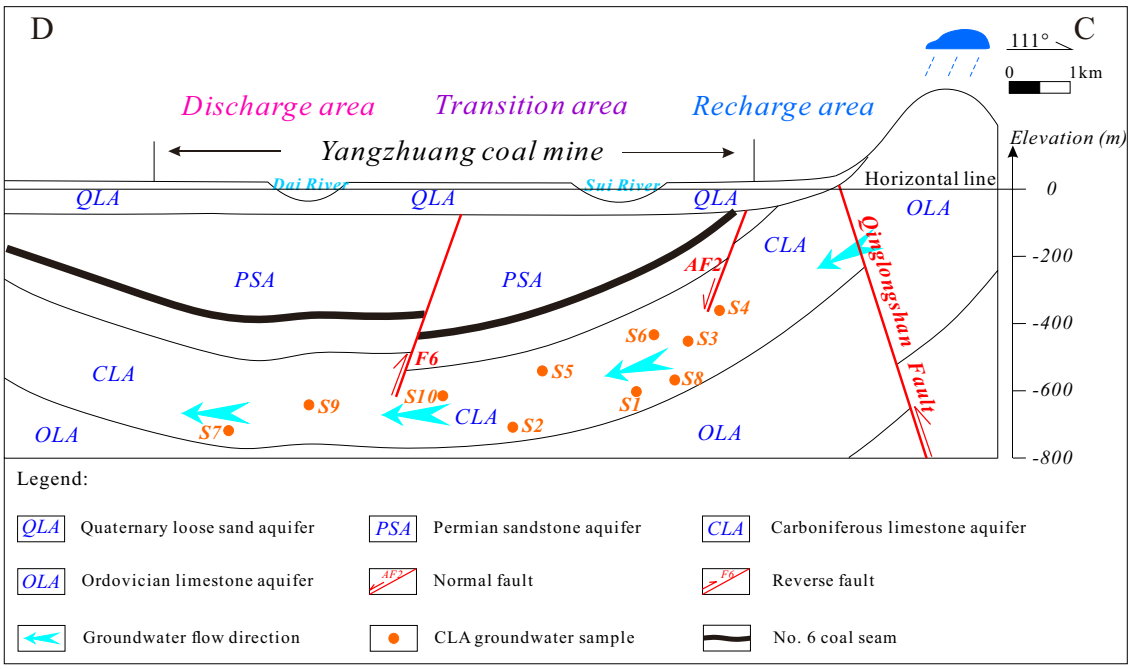

Fig. 2 **C**, **D** cross section and hydrogeological map of the study area. (Note: all sampling points are projection positions on **C**, **D** cross section, see Fig. 1)

In this study, PHREEQC version 3.0 (Parkhurst and Appelo 2013) was used to calculate partial pressures of carbon dioxide (Pco_2) and the saturation index (SI) of potential minerals controlling water–rock interactions. PHREEQC was also used to verify hydrogeochemical processes that occurred along the groundwater flow paths and to confirm deductions based on hydrochemical correlation analysis.

Results and Discussions

General Characteristics of Groundwater

The pH values of the CLA water samples ranged from 7.5 to 7.7 (circumneutral and slightly alkaline). Meanwhile, the TDS ranged from 468 to 713 mg/L, as listed in Table 1, characteristic of freshwater. In all of the water samples, Ca^{2+} and Na^{+} were the dominant cations, and their concentrations ranged from 69.8 to 117.9 mg/L and 31.0 to 120.0 mg/L, respectively. Moreover, Mg^{2+} content was relatively stable with a concentration of 29.9–47.0 mg/L. For anions, the concentration of HCO_3^- ranged from 339.6 to 515.5 mg/L, which has a "high-profile" performance compared with other anions, as listed in Table 1. Sulfate is the second major anion, with a concentration ranging from 81.3 to 203.6 mg/L. The Cl^- ranged from 27.8 to 58.5 mg/L. The Piper tri-linear diagram (Fig. 3) clearly illustrates the three main hydrochemical types: Ca-HCO_3 (S1, S3, S4, S6, S8), Ca·Na-HCO_3 (S2, S5, S10), and Ca·Na-HCO_3·SO_4 (S7, S9).

Q-mode Factor Analysis

SPSS 19.0 software was used to perform Q-factor analysis on 10 selected samples to reveal the internal connection of the samples and facilitate their classification and analysis. Factor 1 accounts for 98.3% of the total variance and contains most of the hydrochemical information with positive high-factor scores for Ca^{2+} and HCO_3^-. Factor 2 exhibits high Na^+, HCO_3^-, and SO_4^{2-} loads and intuitively describes the relationship and change trend among the different samples. Table 2 shows the load value of each sample on factors 1 and 2, which was obtained by using the maximum variance rotation method (Chen et al. 2017). The factor loading diagram shows the change characteristics of the hydrochemistry of all samples, and the results agree well with the Piper tri-linear diagram, as shown in Fig. 4. S1, S3, S4, S6, and S8 (Group A in Fig. 4) are dominated by Ca^{2+} and HCO_3^- with Ca-HCO_3 chemical types, suggesting that these waters were located in an area with good recharge and discharge. As the groundwater shifts deeper in the aquifer, the deterioration of karst fissure development due to increased ground stress worsens the flow conditions and the residence time becomes longer, which gradually complicates

Table 1 Hydrochemical compositions and PHREEQC calculated paraments of the groundwater samples in the study area

Sample ID	T (℃)	pH	Charge balance (%)	TDS (mg/L)	Na^+ (mg/L)	Ca^{2+} (mg/L)	Mg^{2+} (mg/L)	Cl^- (mg/L)	SO_4^{2-} (mg/L)	HCO_3^- (mg/L)	Hydrochemical type	SI_calcite	SI_dolomite	SI_gypsum	Log (Pco_2)
S1	28.8	7.7	0.05	520	43.8	98.4	35.8	43.8	98.9	398.6	Ca-HCO_3	0.87	1.70	− 1.60	− 2.04
S2	29.1	7.7	1.23	536	87.5	69.8	29.9	38.5	103.8	414.0	Ca·Na-HCO_3	0.72	1.47	− 1.70	− 1.98
S3	27.8	7.5	0.21	656	60.6	117.9	46.4	53.3	120.0	515.5	Ca-HCO_3	0.80	1.59	− 1.49	− 1.71
S4	28.5	7.6	0.04	468	31.0	96.0	31.7	43.8	95.9	339.6	Ca-HCO_3	0.72	1.34	− 1.60	− 2.01
S5	30.1	7.6	− 1.84	556	90.0	76.6	34.0	42.7	105.7	414.4	Ca·Na-HCO_3	0.69	1.43	− 1.67	− 1.90
S6	28.6	7.6	1.21	494	57.5	81.4	31.9	37.8	83.0	406.5	Ca-HCO_3	0.70	1.39	− 1.73	− 1.91
S7	30.1	7.7	0.39	671	120.0	79.2	33.1	42.7	181.6	429.7	Ca·Na-HCO_3·SO_4	0.79	1.60	− 1.45	− 1.98
S8	30.9	7.6	− 1.46	608	57.7	111.1	47.0	58.5	81.3	505.9	Ca-HCO_3	0.93	1.90	− 1.67	− 1.81
S9	29.4	7.7	0.88	713	92.5	106.3	39.8	54.6	203.6	433.0	Ca·Na-HCO_3·SO_4	0.93	1.84	− 1.31	− 2.03
S10	29.7	7.6	− 1.08	636	89.1	91.8	40.0	27.8	162.1	450.6	Ca·Na-HCO_3	0.77	1.58	− 1.45	− 1.87

SI (Saturation Index) characterizes the dissolution or precipitation tendency of related minerals in groundwater

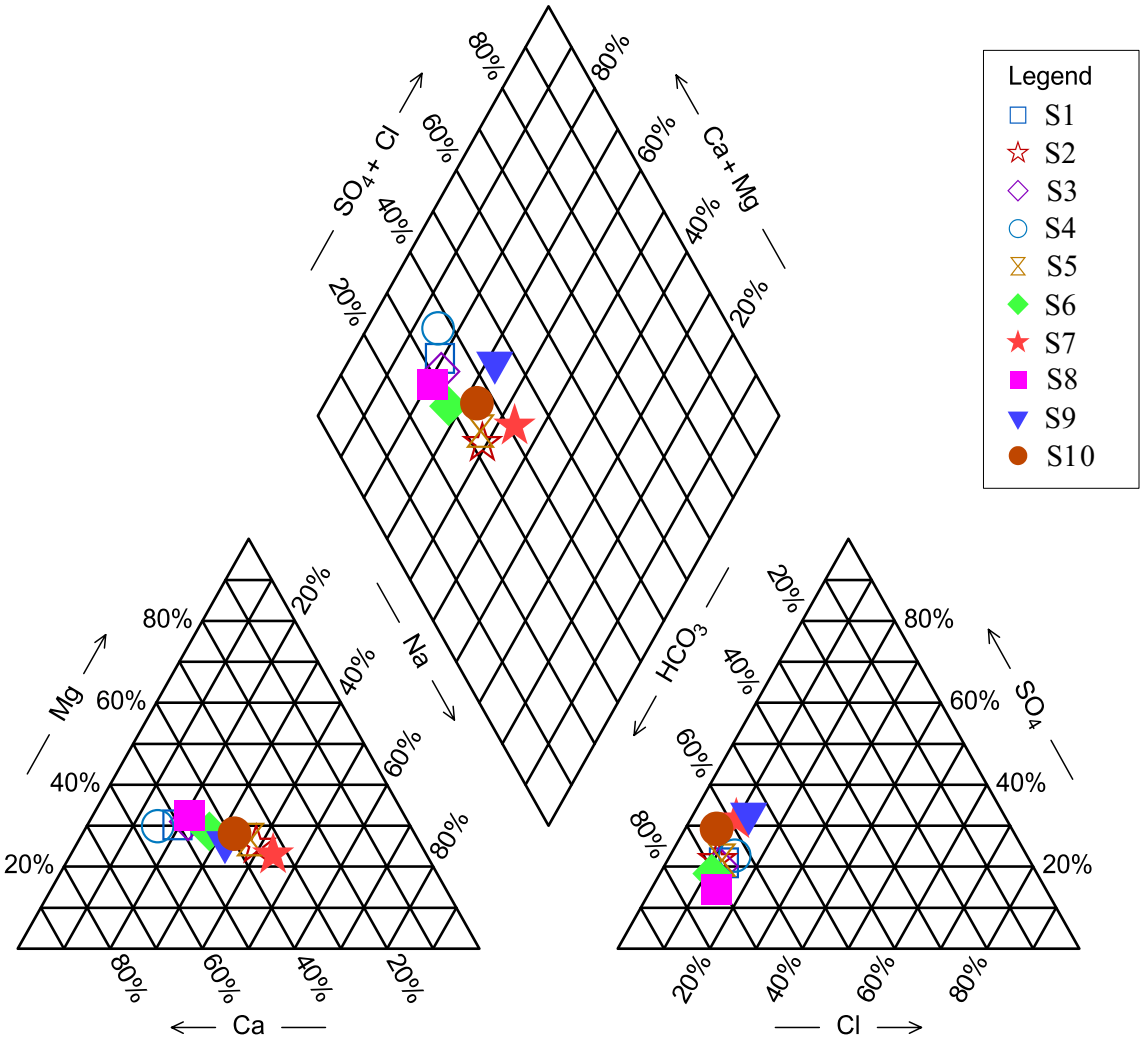

Fig. 3 Piper tri-liner diagram of the groundwater samples from the CLA in the study area

the water's chemical composition. The dominant cation Ca^{2+} is gradually replaced by Na^{+}, and the anion HCO_3^{-} is gradually replaced by SO_4^{2-} or Cl^{-}. Group C contains two water samples, S7 and S9, and are characterized by a Ca·Na-HCO_3·SO_4 type, indicating that the water circulation position should be in the drainage area. Group B is located in the middle and contains three water samples (S2, S5, and S10) that reflect the characteristics of the transitional water quality, mainly corresponding to the Ca·Na-HCO_3 type of water. The diversity of hydrochemical types once again reveals that the hydrogeochemical processes of the Carboniferous groundwater in the study area are complex.

Table 2 Factor loading of groundwater samples in the study area

Label	Hydrochemical type	Factor 1	Factor 2
S1	Ca-HCO_3	0.78	0.62
S2	Ca·Na-HCO_3	0.72	0.69
S3	Ca-HCO_3	0.78	0.62
S4	Ca-HCO_3	0.78	0.62
S5	Ca·Na-HCO_3	0.72	0.69
S6	Ca-HCO_3	0.78	0.62
S7	Ca·Na-HCO_3·SO_4	0.58	0.81
S8	Ca-HCO_3	0.83	0.56
S9	Ca·Na-HCO_3·SO_4	0.60	0.80
S10	Ca·Na-HCO_3	0.66	0.75

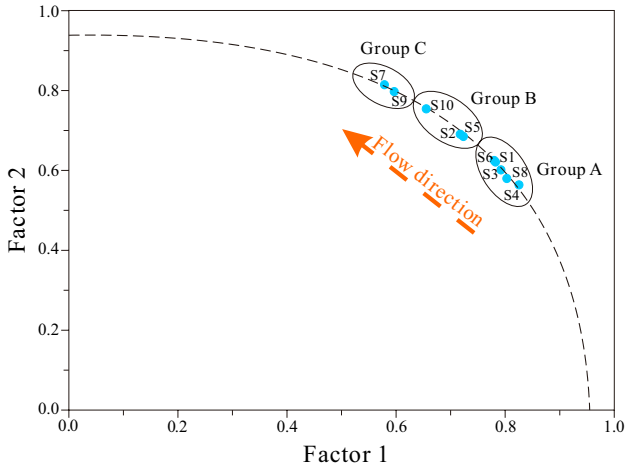

Fig. 4 Q-mode factor analysis for factors 1 and 2. Groups A, B and C respectively represent different hydrochemical components in the flow path, corresponding to Ca-HCO_3 type, Ca·Na-HCO_3 type, and Ca·Na-HCO_3·SO_4 type, respectively

Hydrogeochemical Processes

Potential Mineral Phase

The XRD measurement results, as listed in Table S-1, showed that the minerals controlling the chemical composition of the CLA groundwater in the study area mainly consists of carbonates minerals (such as calcite and dolomite), crystal minerals (such as gypsum and quartz), clay minerals (such as kaolinite), and organic matter (such as carbon) with minor amounts of pyrite and siderite. However, the related test results for water samples from the ICP showed that iron ion concentrations in the water were very small, and some were even less than the detection limit. The dominant ion compositions in the water samples are reactants, such as calcite, dolomite, and gypsum, along with some sodium minerals (e.g., halite). Additionally, due to the presence of carbon in the CLA, desulfurization may occur in a relatively closed reducing environment.

Source of High HCO_3^-

As mentioned above, the HCO_3^- concentration plays a dominant role in groundwater and has a "high-profile" performance compared with other anions. Therefore, identifying the major factors that cause such high levels of HCO_3^- in groundwater was essential for in-depth understanding of the study area's hydrogeochemical processes. Intuitively, the CLA in the study area is a typical limestone aquifer, where carbonate minerals are the likely sources of bicarbonate generation.

According to the calculation results, the $SI_{calcite}$ values in all of the samples ranged from 0.52 to 0.93, while the

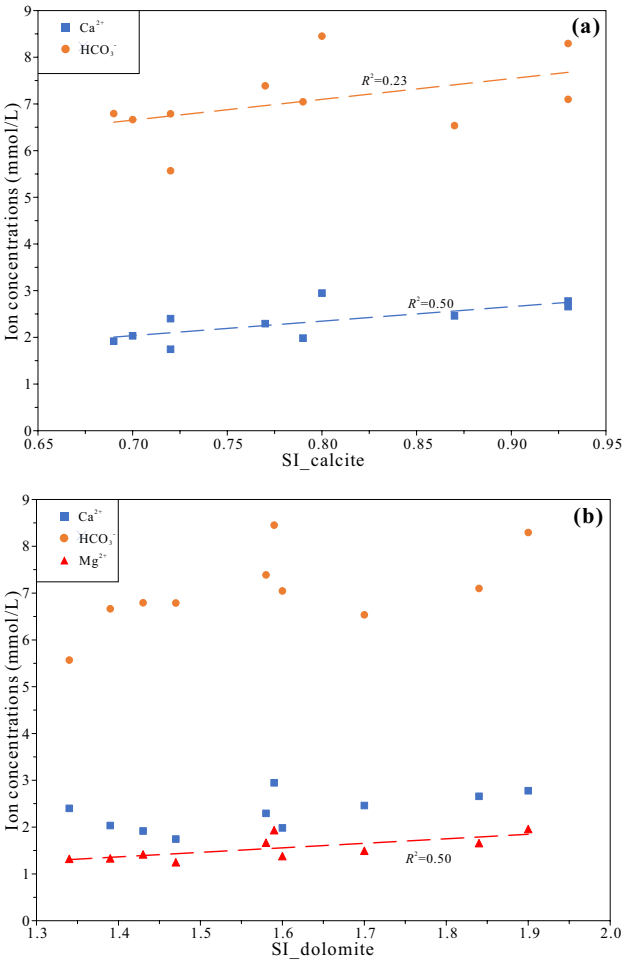

Fig. 5 Relation diagrams of major ions in groundwater samples: **a** correlations of SI_calcite and related ions; b correlations $SI_{dolomite}$ and related ions

$SI_{dolomite}$ value in all samples ranged from 1.34 to 1.90 (Table 1). As shown in Fig. S-1, both $SI_{calcite}$ and $SI_{dolomite}$ were positively associated with TDS, which indicates the release of more Ca^{2+}, Mg^{2+}, and HCO_3^- into the water. It can be seen from Fig. 5a that Ca^{2+} ($R^2 = 0.50$) and HCO_3^- ($R^2 = 0.23$) has a slight correlation with $SI_{calcite}$. The same is true for $SI_{dolomite}$ (Fig. 5b), only Mg^{2+} ($R^2 = 0.50$) has a relatively good correlation with $SI_{dolomite}$. Since the values of $SI_{calcite}$ in all of the samples were greater than 0, precipitation was indicated, but the situation is still far from supersaturated. Given the variation trends of ions in water, it can be inferred that these characteristics may be due to differences in dissolution rates of calcite and dolomite and other groundwater processes that affect the concentration of Ca^{2+}, such as cation exchange.

$$\text{Calcite}: CaCO_3 + CO_2(g) + H_2O \rightarrow Ca^{2+} + 2\,HCO_3^- \quad (1)$$

$$\text{Dolomite}: \ CaMg(CO_3)_2 + 2\,CO_2 + 2\,H_2O \rightarrow Ca^{2+} + Mg^{2+} + 4\,HCO_3^- \quad (2)$$

The molar ratio of HCO_3^- to Ca^{2+} directly reflects a variety hydrogeochemical processes, including the dissolution of carbonate minerals, cation exchange, and/or sulfate reduction. If the groundwater's chemistry consisted of ions coming solely from the dissolution of calcite, the ratio of HCO_3^-/Ca^{2+} would be 2, whereas if it was from the dissolution of dolomite, the ratio would be 4 (Eqs. (1) and (2)). Figure 6 shows the scatter plot of the two ions, which were subdivided into three regions by two constant ratio lines of $y = 2x$, and $y = 4x$. The upper region represents the concentration of $HCO_3^- > 4 \times Ca^{2+}$. If the major origins of Ca^{2+}, Mg^{2+}, and HCO_3^- in water are from the two carbonate minerals, the upper region can be affected by cation exchange. And if the HCO_3^- comes from more than mineral dissolution, then it could also indicate sulfate reduction. As mentioned above, some organic carbon is present. However, no sample was located in this region, indicating that sulfate reduction, if it is occurring at all, is not significant. The middle part is a transition region, representing calcite and dolomite dissolution or calcite dissolution and the participation of Ca^{2+} in cation exchange. All of the samples are located in this area, which suggests that the carbonate in the study area is in a dissolved state and bicarbonate has been produced, though it does not exclude cation exchange. The lower region shows HCO_3^- deficiency, and no samples fell in this area.

Generally, there are open and closed carbonate systems in natural groundwater. For a closed system, CO_2 will be insufficient because it is consumed and cannot be replenished, whereas the reverse is the case in an open system (Shen et al. 1999). Groundwater in an open carbonate system tends to have significantly higher bicarbonate concentrations. Langmuir (1997) defined the system's opening or closing by the difference between the P_{CO2} and the atmosphere.

The Pco_2 of all water samples were calculated by PHREEQC version 3.0 software, and the results showed that the Log (P_{CO_2}) of all samples was greater than in the atmosphere with a value of -3.5 bar, indicating that the study area has an open carbonate system. Figure 7 shows the scatter plot between Pco_2 and bicarbonate concentration. It can be clearly seen that there is a significantly positive correlation between these two parameters. The more CO_2 the system contains, the higher the bicarbonate concentration.

From the perspective of geological stratigraphy, the CLA is a deep confined aquifer at the bottom of the Permian, which should belong to a closed system under normal conditions. However, the cross-section in Fig. 2 clearly explains why the system is only slightly closed. The Yangzhuang coal mine is located at the southern end of the Zhahe syncline, and the overall geological structure is an asymmetric syncline with a NE axis. The Ordovician strata are exposed southeast of the coal mine, and directly receive the recharge of atmospheric precipitation. The CLA and OLA are hydraulically connected through the Qinglongshan thrust fault and multiple oblique faults. Furthermore, due to the high pressure, the Carboniferous groundwater in the mining area may flow into the coal tunnel through the small fault fracture zones and mining fractures. In 1988, the Yangzhuang mine experienced a huge water-inrush disaster due to the faulty zone connecting the Carboniferous groundwater (Luo and Peng 2005; Wang et al. 2009). In recent years, underlying aquifer disasters from the CLA have also occurred frequently, and the water gushing channels are fault fracture zones and mining fractures. Moreover, similar to most north China coal mines, the Yangzhuang mine uses drainage to reduce the hazards of underlying aquifer disasters, which has

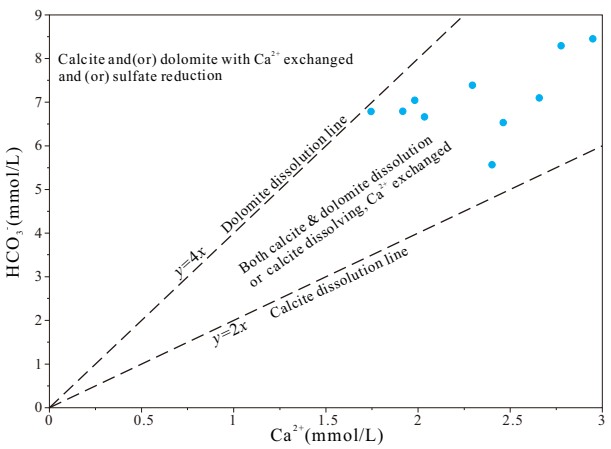

Fig. 6 Scatter plot of Ca^{2+} and HCO_3^- in groundwater samples

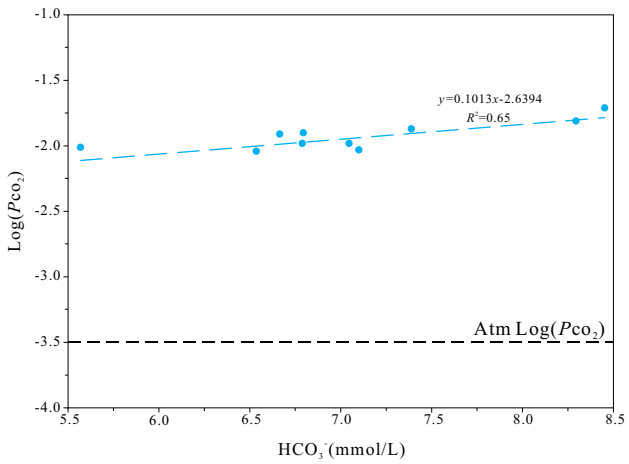

Fig. 7 Scatter plot of HCO_3^- and log (P_{CO_2}). The dashed line corresponds to the atmospheric partial pressure of CO_2

caused the groundwater level of the CLA to decrease year by year (Fig. S-2, water-table data were collected on Dec. 31st of every year). All these situations indicate that the CLA in the study area is only relatively closed.

Source of SO_4^{2-}

The origins of dissolved SO_4^{2-} in groundwater are relatively complex but mainly include: the dissolution of evaporitic minerals with gypsum; the oxidation of sulfide minerals; atmospheric acid deposition; emissions of industrial and domestic wastewater, coal mining activities, and other anthropogenic contaminants. In this study, sulfate is a secondary high-concentration anion in the target groundwater layers. The XRD testing results show that gypsum exists in the Carboniferous formations, which may be the source of sulfate in groundwater. Due to the extremely low concentration of Fe in the groundwater, sulfide mineral oxidation was not considered a major SO_4^{2-} source.

The SI_{gypsum} in all groundwater samples was less than 0, ranging from − 1.73 to − 1.31, with an average value of − 1.57, indicating that the gypsum remains dissolved along the flow path. Fig. S-1 shows that there is a significant correlation between SI_{gypsum} and TDS ($R^2 = 0.66$). If the hydrochemistry of Ca^{2+} and SO_4^{2-} is mainly contributed by gypsum dissolution, the ratio of SO_4^{2-}/Ca^{2+} should be a constant value of 1:1, as defined in Eq. 3. Figure 8 is a scatter plot of the two gypsum ions. As can be seen, all samples are below the constant ratio line, and the concentrations of Ca^{2+} are higher than that of SO_4^{2-}. This suggests that the major source of calcium is the dissolution of carbonate minerals. There is a significant correlation between SO_4^{2-} and SI_{gypsum} ($R^2 = 0.85$; Fig. 9), but there is no clear relationship between Ca^{2+} and SI_{gypsum}, which verifies that gypsum continues to dissolve along the flow path and release SO_4^{2-}. The distributed feature also explains the hydrogeochemical processes of Ca^{2+} in groundwater, which includes carbonate mineral dissolution and cation exchange.

$$\text{Gypsum}: \ CaSO_4 \cdot 2\,H_2O = Ca^{2+} + SO_4^{2-} + 2\,H_2O \tag{3}$$

Evidence of cation exchange

Generally, Cl^- is considered to be a highly soluble conservative ion that is not absorbed by plants, bacteria, and soil surface particles, and that is not easy to precipitate. Therefore, the molar ratio of Na^+/Cl^- is often used to determine the source of Na^+ in groundwater. If Na^+ and Cl^- were only derived from halite dissolution, the molar ratio of Na^+/Cl^- should be 1. As shown in Fig. 10a, all samples plot below the 1:1 line, indicating that cation exchange is

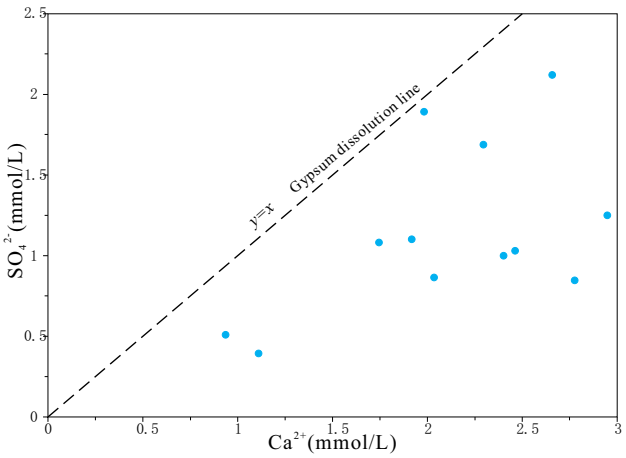

Fig. 8 Scatter plot of Ca^{2+} and SO_4^{2-}

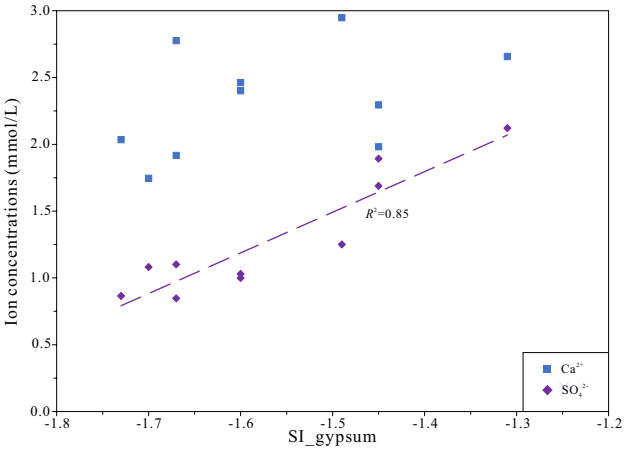

Fig. 9 Relation diagram of SI_{gypsum} and related ions

also taking place. If the dissolution of corresponding minerals mainly consists Na^+, Ca^{2+}, and Mg^{2+}, then the ratio of $(Na^+\text{-}Cl^-)/(Ca^{2+} + Mg^{2+}\text{-}SO_4^{2-}\text{-}HCO_3^-)$ in the unit of meq/L will be a constant 1:1. The scattering distribution in Fig. 10b also indicates that ion exchange has occurred, which is consistent with the previous discussion. Figure 10c shows that Ca^{2+} and Mg^{2+} are both deficient compared with SO_4^{2-} and HCO_3-. Considering the general order of affinity among different cations, Ca^{2+} is generally preferred over Mg^{2+} in most cases (Liu et al. 2017). Therefore, it is speculated that Ca^{2+} is the major ion involved in cation exchange. The direction of the exchange may be the adsorption of Ca^{2+} and the desorption of Na^+, as described in Eq. 4, where X is the exchange complex. Schoeller (1965) suggested that by studying the chlor-alkali indices (Eqs. 5 and 6), the ion exchange between the groundwater and the host environment can be understood. Negative indices mean that Ca^{2+}/Mg^{2+} has been removed from solution and replaced by Na^+/K^+,

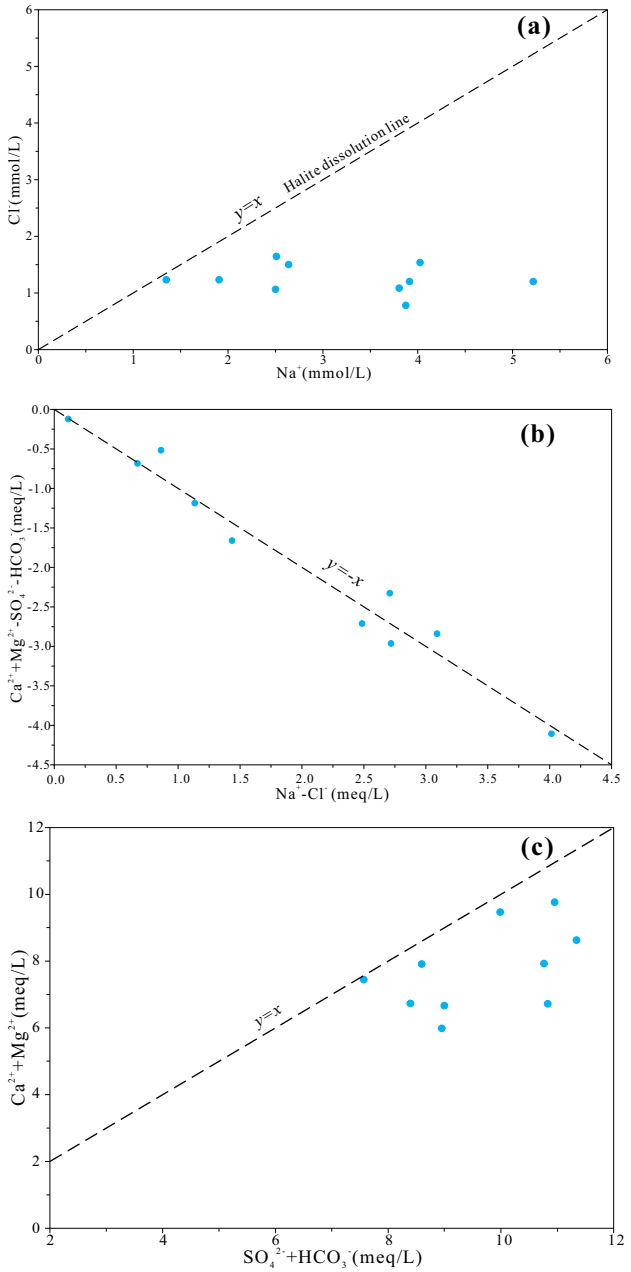

Fig. 10 Plot showing the relationship between **a** Na^+ and Cl^-, **b** $Ca^{2+}+Mg^{2+}$-SO_4^{2-}–HCO_3^- and Na^+-Cl^-, and **c** $Ca^{2+}+Mg^{2+}$ and $SO_4^{2-}+HCO_3^-$

whereas positive values indicate reverse reactions have taken place. After calculating all samples in the Yangzhuang mine using the Schoeller formulas, the results show that the value of CAI-I ranges from -3.95 to -0.09, with an average value of − 1.69, while the value of CAI-II ranges from -0.37 to -0.01 (avg. -0.19), indicating that cation exchange has occurred in the CLA groundwater.

$$2\,NaX + Ca^{2+} \rightarrow CaX_2 + 2\,Na^+ \quad (4)$$

$$CAI - I = \left[Cl^- - \left(Na^+ + Cl^-\right)\right] / Cl^- \quad (5)$$

$$CAI - II = \left[Cl^- - \left(Na^+ + Cl^-\right)\right] / \left(HCO_3^- + SO_4^{2-} + CO_3^{2-} + NO_3^-\right) \quad (6)$$

Inverse Geochemical Modeling

In this study, inverse geochemical modeling was used to verify the processes inferred from the previous results. The specific reactants and reactions involved in this hydrogeochemical process are shown in Table S-2. Two lines were selected to illustrate the hydrogeochemical process in the groundwater path. Line 1 was used to explain a series of main processes that take place in the flow path in detail, and line 2 was used as a parallel model of line 1, mainly to verify its correctness.

Line 1: Combining the actual geological conditions of the study area and the sampling location (Fig. 2), two water samples (S4 and S9) along the flow path were selected as the initial and final solution (Table S-3; locations are shown in Fig. 2). After calculation, PHREEQC found that only one possible model was suitable for modeling the process (Table 3). The inverse model is consistent with the previous speculation that calcite and dolomite may still be dissolving. The solubility of calcite seems to be slightly stronger than that of dolomite, with respect to calcite molality transfer $3.59e^{-4}$ mol/L and dolomite $1.58e^{-4}$ mol/L.

It is worth noting that the molality transfer of gypsum ($1.04e^{-3}$ mol/L) is greater than that of calcite and dolomite, which is consistent with gypsum dissolution and explains the relatively high concentrations of SO_4^{2-} in the water samples.

Given that the carbonate and gypsum are dissolving, the concentrations of Ca^{2+} in the water samples should accumulate along the flow path. However, it can be seen from Table S-3 that, compared with the initial solution, the concentration of Ca^{2+} in the final solution only increased by 10 mg/L, which was much less than the SO_4^{2-}. Cation exchange involving sodium and calcium is the main reason for this. CaX2 adsorbs Ca^{2+} with a negative value at a molar transfer rate of $-1.28e^{-3}$ mol/L, whereas the reverse is true for Na^+, which has desorbed at a molar transfer rate of $2.57e^{-3}$ mol/L. Therefore, a large amount of NaX and Ca^{2+} is involved in cation exchange, significantly increasing the concentration of Na^+ in solution. The small increase in Ca^{2+} indicates that the total amount of Ca^{2+} produced by the dissolution of carbonates and gypsum is slightly greater than the amount consumed by cation exchange. Cl^- and Mg^{2+} also slightly increase along the flow path, mainly

Table 3 Inverse geochemical modeling calculation results of line 1 (units in mol/L)

Phase	Chemical composition	Flow path: S4 → S9	
		Mole transfer	Process indicated from the inverse model
Calcite	$CaCO_3$	$3.599e^{-4}$	Dissolution
CaX2	CaX_2	$-1.283e^{-3}$	Adsorption Ca
Gypsum	$CaSO_4{\cdot}2H_2O$	$1.044e^{-3}$	Dissolution
NaX	NaX	$2.565e^{-3}$	Desorption Na
$CO_2(g)$	$CO_2(g)$	$8.107e^{-4}$	Dissolution
Halite	NaCl	$3.024e^{-4}$	Dissolution
Dolomite	$CaMg(CO_3)_2$	$1.580e^{-4}$	

due to dissolution of the corresponding minerals (dolomite and halite); the molar transfer rates are $3.02e^{-4}$ mol/L and $3.56e^{-4}$ mol/L, respectively.

Line 2 is another section, implemented to verify the correctness of line 1 and to interpret some details that may not have been revealed by line 1. The water chemistry of samples S6 and S7 (chemical compositions listed in Table S-4) were used in the inverse modeling, and the results are shown in Table 4.

After calculation, PHREEQC produced two different models. Among them, model A is consistent with the processes revealed by line 1, though only a small amount of dolomite was dissolved. Model B provides another possibility that no dolomite dissolved along the flow path because the concentration of Mg^{2+} in the two solutions changes very little, and the remaining results are the same as model A.

Conceptual Model

The evolutionary mechanism of groundwater quality and flow can be described by the conceptual model shown in Fig. 11. Carboniferous groundwater receives recharge from Ordovician groundwater through faults in the southeast and flows to the northwest. The TDS concentrations of the samples tend to increase gradually from the southeastern areas to the coal-mining regions, which indicates the accumulating process of ions along the groundwater flow paths. Ca-HCO_3 is the dominant water chemical type of groundwater in the recharge area. Carbonate minerals and gypsum are dissolved along the flow path, accompanied by cation exchange. These processes control the chemical compositions in the water. The groundwater gradually changes to Ca·Na-HCO_3 type, and finally, becomes Ca·Na-$HCO_3{\cdot}SO_4$ type in the discharge area. Additionally, it is noted that halite is well dissolved, although there is no large amount being consumed, which explains the low chlorine concentrations in the water samples. The aquifer rock is believed to contain a limited amount of halite.

Conclusions

This study investigated the main processes controlling the hydrogeochemical characteristics of the CLA in the Yangzhuang coal mine, Anhui Province using multivariate statistics, chemical correlation analysis, and inverse geochemical modeling. From the results, the following conclusions can be summarized.

Table 4 Inverse geochemical modeling calculation results of line 2 (units in mol/L)

Phase	Chemical composition	Flow path: S6 → S7			
		Model A		Model B	
		Mole transfer	Process indicated from the inverse model	Mole transfer	Process indicated from the inverse model
Calcite	$CaCO_3$	$2.720e^{-4}$	Dissolution	$2.982e^{-4}$	Precipitation
CaX2	CaX_2	$-1.355e^{-3}$	Adsorption Ca	$-1.368e^{-3}$	Desorption Ca
Gypsum	$CaSO_4{\cdot}2H_2O$	$9.735e^{-4}$	Dissolution	$9.735e^{-4}$	Dissolution
NaX	NaX	$2.711e^{-3}$	Desorption Na	$2.737e^{-3}$	Adsorption Na
$CO_2(g)$	$CO_2(g)$	$2.210e^{-4}$	Dissolution	$2.210e^{-4}$	Dissolution
Halite	NaCl	$1.513e^{-4}$	Dissolution	$1.251e^{-4}$	Dissolution
Dolomite	$CaMg(CO_3)_2$	$1.309e^{-5}$	Dissolution	–	–

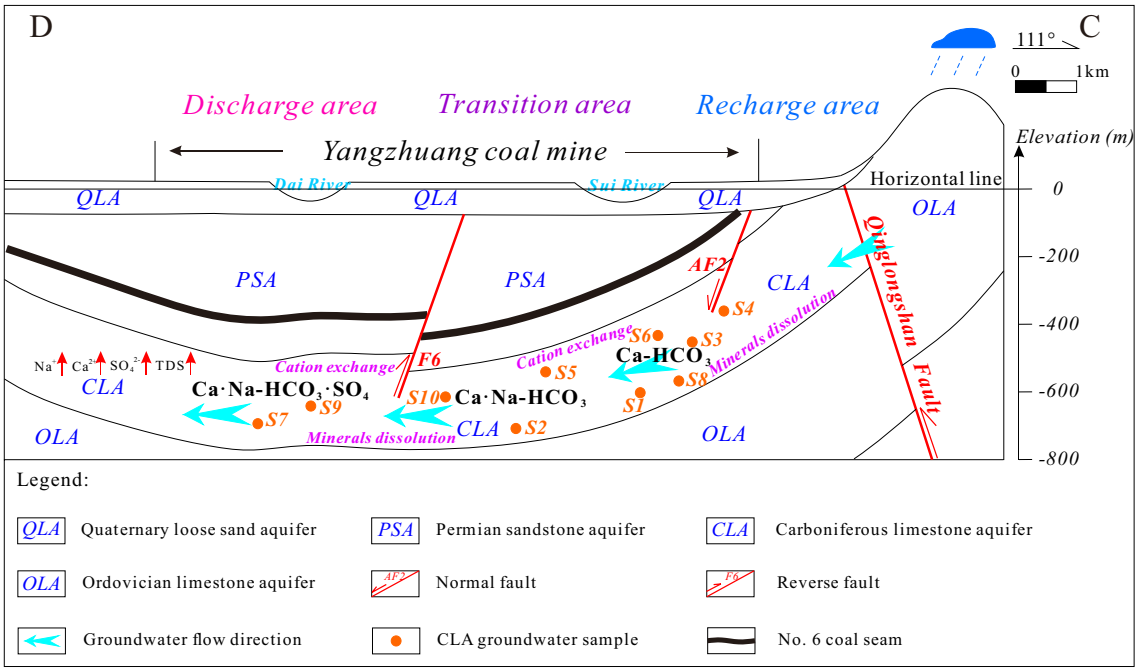

Fig. 11 Hydrogeological conceptual model of the CLA in the Yangzhuang coal mine. Along the groundwater flow direction, the dissolution of carbonate minerals and gypsum together with cation exchange controls the groundwater's hydrochemical evolution

1. The dominant cations in the Carboniferous groundwater in the study area are Ca^{2+} and Na^{+}, and the anion is HCO_3^{-}. The three hydrochemical types reveal differences in groundwater chemical composition at different locations along the flow path. Q-mode factor analysis explained the evolution of the groundwater hydrochemistry accurately. In the direction of flow, the Na^{+} and SO_4^{2-} concentrations gradually increase and the hydrochemical type transforms from Ca-HCO_3 to Ca·Na-HCO_3 and Ca·Na-HCO_3·SO_4.
2. There are two reasons for the high bicarbonate concentration. One is the dissolution of carbonate minerals. Ion correlation analysis suggests that calcite and dolomite may still be dissolving, with calcite doing so slightly more than dolomite. The other is the open carbonate system. After calculation, the Pco_2 of all samples showed obvious openness. Frequent water inrush events and declining water levels due to groundwater extraction provide more evidence for the Carboniferous limestone aquifer being only partially closed.
3. The unbalanced molar ratio of Na^{+} and Cl^{-} and the negative chlor-alkali index of all samples is induced by cation exchange within the groundwater. Similarly, the unbalanced molar ratio of Ca^{2+} and SO_4^{2-} and the excellent correlation between SI_{gypsum} and SO_4^{2-} indicate that SO_4^{2-} is mainly derived from gypsum dissolution.
4. Inverse geochemical modeling of the two paths successfully confirmed the previous speculation. Both calcite and dolomite are partially dissolved, and calcite is slightly soluble than dolomite. The gypsum is in an unsaturated state and continues to dissolve, resulting in SO_4^{2-} being the second-highest anion in water. Cation exchange is occurring, with Ca^{2+} being adsorbed and Na^{+} being desorbed. Cl^{-} comes from the dissolution of the limited amount of halite in the aquifer rock, resulting in only a slight increase in the concentration of Cl^{-}.

Supplementary Information The online version contains supplementary material available at https://doi.org/10.1007/s10230-022-00861-y.

Acknowledgements This work was funded by the National Natural Science Foundation of China (NSFC) (Grants 41972256, 41372244). We also thank the kind reviewers and editors for their considerable work.

References

Adam PJ, Paul LY (2000) Broadening the scope of mine water environmental impact assessment: a UK perspective. Environ Impact Assess Rev 20:85–96

Adhikari K, Mal U (2019) Application of multivariate statistics in the analysis of groundwater geochemistry in and around the open cast coal mines of Barjora block, Bankura district, West Bengal. India Environ Earth Sci 78:72

Andreas K, Nikola R (2011) Special issue: sustainable development of energy, water and environment systems. Water Resour Manag 25:2917–2918

Binet S, Joigneaux E, Pauwels H, Alberic P, Flehoc C, Bruand A (2016) Water exchange, mixing and transient storage between a saturated karstic conduit and the surrounding aquifer: groundwater flow modeling and inputs from stable water isotopes. J Hydrol 544:278–289

Bridge G (2004) Contested terrain: mining and the environment. Annu Rev Environ Resour 29:205–259

Carucci V, Petitta M, Aravena R (2012) Applied Geochemistry Interaction between shallowand deep aquifers in the Tivoli Plain (Central Italy) enhanced by groundwater extraction: a multi-isotope approach and geochemical modeling. Appl Geochem 27(1):266–280

Chen LW, Feng XQ, Xie WP, Xu DQ (2016) Prediction of water-inrush risk areas in process of mining under the unconsolidated and confined aquifer: a case study from the Qidong coal mine in China. Environ Earth Sci 75:706

Chen LW, Xie WP, Feng XQ, Zhang NQ, Yin XX (2017) Formation of hydrochemical composition and spatio-temporal evolution mechanism under mining-induced disturbance in the Linhuan coal-mining district. Arab J Geosci 10:57

Cortes JE, Muñoz LF, Gonzalez CA, Niño JE, Polo A, Suspes A, Trujillo HL (2016) Hydrogeochemistry of the formation waters in the San Francisco field, UMV basin, Colombia—a multivariate statistical approach. J Hydrol 539:113–124

Davis JC (1973) Statistics and data analysis in geology. Wiley, New York

Dogramaci S, McLean L, Skrzypek G (2017) Hydrochemical and stable isotope indicators of pyrite oxidation in carbonate-rich environment; the Hamersley Basin, Western Australia. J Hydrol 545:288–298

Gastmans D, Chang HK, Hutcheon I (2010) Groundwater geochemical evolution in the northern portion of the Guarani Aquifer System (Brazil) and its relationship to diagenetic features. Appl Geochem 25(1):16–33

Gui HR, Song XM, Lin ML (2017) Water-inrush mechanism research mining above karst confined aquifer and applications in North China coalmines. Arab J Geosci 10:180

Güler C, Thyne GD, McCray JE, Turner AK (2002) Evaluation of graphical and multivariate statistical methods for classification of water chemistry data. Hydrogeol J 10:455–474

Güler C, Kurt MA, Alpaslan M, Akbulut C (2012) Assessment of the impact of anthropogenic activities on the groundwater hydrology and chemistry in Tarsus coastal plain (Mersin, SE Turkey) using fuzzy clustering, multivariate statistics and GIS techniques. J Hydrol 414–415:435–451

Han Y, Wang GC, Cravotta CA III, Hu WY, Bian YY, Zhang ZW, Liu YY (2013) Hydrogeochemical evolution of Ordovician limestone groundwater in Yanzhou, North China. Hydrol Process 27(16):2247–2257

Hu WY, Yan LY (2000) Characteristics of groundwater pollution in abandon coal mine and control technique (in Chinese). Coal Mine Environ Prot 14(4):37–38

Huang PH, Chen JS (2012) Recharge sources and hydrogeochemical evolution of groundwater in the coal-mining district of Jiaozuo, China. Hydrogeol J 20:739–754

Huang H, Lu J (2014) Identification of river water pollution characteristics based on projection pursuit and factor analysis. Environ Earth Sci 72:3409–3417

Johnson KL, Younger PL (2006) The co-treatment of sewage and mine waters in aerobic wetlands. Eng Geol 85(1–2):53–61

Kanduč T, Grassa F, Mclntosh J, Stibilj V, Ulrich-Supovec M, Supovec I, Jamnikar S (2014) A geochemical and stable isotope investigation of groundwater/surface-water interactions in the Velenje Basin, Slovenia. Hydrogeol J 22:971–984

Langmuir D (1997) Aqueous environmental geochemistry. Prentice-Hall, Englewood Cliffs, NJ, pp 193–230

Li QG, Wu P, Zha XF, Li XX, Wu LN, Gu SY (2018) Effects of mining activities on evolution of water chemistry in coal-bearing aquifers in karst region of Midwestern Guizhou, China: evidences from $\delta^{13}C$ of dissolved inorganic carbon and $\delta^{34}S$ of sulfate. Environ Sci Pollut Res 25:18038–18048

Liang YP, Gao XB, Zhao CH, Tang CL, Shen HY, Wang ZH, Wang YX (2018) Review: Characterization, evolution, and environmental issues of karst water systems in northern China. Hydrogeol J 26:1371–1385

Lin Y, Ren HX, Wu YZ, Cao FL, Jia FJ, Qu PC (2019) The evolution of hydrogeochemical characteristics of a typical piedmont karst groundwater system in a coal-mining area, northern China. Environ Earth Sci 78:557

Liu P, Sun YJ (2011) Discussion on groundwater pollution caused by abandoned mines and its controlling techniques (in Chinese). Min Res Dev 31(4):91–95

Liu P, Hoth N, Drebenstedt C, Sun YJ, Xu ZM (2017) Hydro-geochemical paths of multi-layer groundwater system in coal mining regions—using multivariate statistics and geochemical modeling approaches. Sci Total Environ 601–602:1–14

Liu F, Wang S, Wang LS, Shi LM, Song XF, Yeh T-CJ, Zhen PN (2019a) Coupling hydrochemistry and stable isotopes to identify the major factors affecting groundwater geochemical evolution in the Heilongdong Spring Basin. North China. J Geochem Explor 205:106352

Liu P, Yang M, Sun YJ (2019b) Hydro-geochemical processes of the deep Ordovician groundwater in a coal mining area, Xuzhou, China. Hydrogeol J 27:2231–2244

Liu F, Zhao ZP, Yang LH, Ma YX, Xu YC, Gong L, Liu HY (2020) Geochemical characterization of shallow groundwater using multivariate statistical analysis and geochemical modeling in an irrigated region along the upper Yellow River. Northwestern China. J Geochem Explor 215:106565

Luo LP, Peng SP (2005) Mechanism study on water-inrush hazard of floor strata in mining on confined aquifer. J China Coal Soc 30(4):459–462 (**in Chinese**)

Ma R, Wang YX, Sun ZY, Zheng CM, Ma T, Prommer H (2011) Geochemical evolution of groundwater in carbonate aquifers in Taiyuan, northern China. Appl Geochem 26(5):884–897

Ministry of Water Resources of China (2019) Water Resources Bulletin. China Northern Plains. Beijing, Ministry of Water Resources of China, http://www.mwr.gov.cn/. Accessed 15 July 2020

Moya CE, Raiber M, Taulis M, Cox ME (2016) Using environmental isotopes and dissolved methane concentrations to constrain hydrochemical processes and inter-aquifer mixing in the Galilee and Eromanga Basins, Great Artesian Basin, Australia. J Hydrol 539:304–318

National Bureau of Statistics of China (2019) National Economic and Social Development Statistical Bulletin. Total energy consumption. Beijing, National Bureau of Statistics of China, https://data.stats.gov.cn/easyquery.htm. Accessed 23 Aug 2020

Parkhurst DL, Appelo CAJ (2013) Description of input and examples for PHREEQC version 3—a computer program for speciation, batch-reaction, one dimensional transport, and inverse geochemical calculations. Chapter 43 of Section A, Groundwater Book 6, Modeling Techniques, http://pubs.usgs.gov/tm/06/a43/. Accessed 5 May 2018

Qian JZ, Wang L, Ma L, Lu YH, Zhao WD, Zhang Y (2016) Multivariate statistical analysis of water chemistry in evaluating groundwater geochemical evolution and aquifer connectivity near a large coal mine, Anhui China. Environ Earth Sci 75:747

Qian JZ, Tong Y, Ma L, Zhao WD, Zhang RG, He XR (2018) Hydrochemical characteristics and groundwater source identification of a multiple aquifer system in a coal mine. Mine Water Environ 37:528–540

Qiao W, Li WP, Zhang SC, Niu YF (2019) Effects of coal mining on the evolution of groundwater hydrogeochemistry. Hydrogeol J 27:2245–2262

Qu S, Wang GC, Shi ZM, Xu QY, Guo YY, Ma L, Sheng YZ (2018) Using stable isotopes (δD, $\delta^{18}O$, $\delta^{34}S$ and $^{87}Sr/^{86}Sr$) to identify sources of water in abandoned mines in the Fengfeng coal mining district, northern China. Hydrogeol J 26:1443–1453

Salmi EF, Nazem M, Karakus M (2017) Numerical analysis of a large landslide induced by coal mining subsidence. Eng Geol 217:141–152

Schoeller H (1965) Qualitative evaluation of groundwater resources. In: Methods and techniques of groundwater investigation and development. Water Research, Series-33. UNESCO, pp 54–83

Sefie A, Aris AZ, Ramli MF, Narany TS, Shamsuddin MKN, Saadudin SB, Zali MA (2018) Hydrogeochemistry and groundwater quality assessment of the multilayered aquifer in Lower Kelantan Basin, Kelantan, Malaysia. Environ Earth Sci 77:397

Shen ZL, Zhu WH, Zhong ZS (1999) Hydrogeochemistry basics (in Chinese). Geology Press, Beijing, pp 101–110

Shi LQ, Qiu M, Wang Y, Qu XY, Liu TH (2019) Evaluation of water inrush from underlying aquifers by using a modified water-inrush coefficient model and water-inrush index model: a case study in Feicheng coalfield, China. Hydrogeol J 27:2105–2119

Sun J, Kobayashi T, Strosnider WHJ, Wu P (2017) Stable sulfur and oxygen isotopes as geochemical tracers of sulfate in karst waters. J Hydrol 551:245–252

Szabó NP (2015) Hydraulic conductivity explored by factor analysis of borehole geophysical data. Hydrogeol J 23:869–882

Trabelsi R, Zouari K (2019) Coupled geochemical modeling and multivariate statistical analysis approach for the assessment of groundwater quality in irrigated areas: A study from North Eastern of Tunisia. Groundw Sustain Dev 8:413–427

Unlu T, Akcin H, Yilmaz O (2013) An integrated approach for the prediction of subsidence for coal mining basins. Eng Geol 166:186–203

Walden J, Smith JP, Dackombe RV (1992) The use of simultaneous R- and Q-mode factor analysis as a tool for assisting interpretation of mineral magnetic data. Math Geol 24(3):227–247

Wang CS, Sun YJ, Hang Y (2009) Application of fault tree analysis to risk assessment of potential water-inrush hazards in coal mining (in Chinese). Chin J Rock Mech Eng 28(2):298–305

Wu Q, Fan ZL, Zhang ZW, Zhou WF (2014) Evaluation and zoning of groundwater hazards in Pingshuo no. 1 underground coal mine, Shanxi Province. China Hydrogeol J 22:1693–1705

Wu Q, Guo XM, Shen JJ, Xu S, Liu SQ, Zeng YF (2017) Risk assessment of water inrush from aquifers underlying the Gushuyuan Coal Mine, China. Mine Water Environ 36:96–103

Xue X, Wu JW, Wang HZ (2014) Research on sedimentary characteristics of Taiyuan formation limestone in Huaibei coalfield. China Energy Environ Prot 11:102–105 (**in Chinese**)

Yin D, Shu LC, Chen XH, Wang ZL, Mohammed ME (2011) Assessment of sustainable yield of Karst Water in Huaibei, China. Water Resour Manag 25:287–300

Yin HY, Zhao H, Xie DL, Sang SZ, Shi YL, Tian MH (2019) Mechanism of mine water inrush from overlying porous aquifer in Quaternary: a case study in Xinhe Coal Mine of Shandong Province China. Arab J Geosci 12:163

Younger PL, Wolkersdorfer C (2004) Mining impacts on the fresh water environment: technical and managerial guidelines for catchment scale management. Mine Water Environ 23(Suppl 1):s2–s80

Zhang JC (2005) Investigations of water inrushes from aquifers under coal seams. Int J Rock Mech Min Sci 42:350–360

Zhang HT, Xu GQ, Zhan HB, Chen XQ, Liu MC, Wang MH (2020a) Identification of hydrogeochemical processes and transport paths of a multi-aquifer system in closed mining regions. J Hydrol 589:125344

Zhang J, Chen LW, Chen YF, Ge RT, Ma L, Zhou KD, Shi XP (2020b) Discrimination of water-inrush source and evolution analysis of hydrochemical environment under mining in Renlou coal mine, Anhui Province, China. Environ Earth Sci 79:61

Zhang J, Chen LW, Li J, Chen YF, Ren XX, Shi XP (2021) Analysis of mining effects on the geochemical evolution of groundwater, Huaibei coalfield, China. Environ Earth Sci 80:98

Zheng LG, Chen X, Dong XL, Wei XP, Jiang CL, Tang Q (2019) Using δ34S–SO4 and δ18O–SO4 to trace the sources of sulfate in different types of surface water from the Linhuan coal-mining subsidence area of Huaibei, China. Ecotoxicol Environ Saf 181:231–240